Optical Pulse Compression Reflectometry Based on Double Sideband Modulation

Lei Yu, Weiwen Zou, *Senior Member, IEEE*, and Jianping Chen

***Abstract*— We propose a novel scheme of optical pulse compression reflectometry (OPCR) based on double sideband modulation (DSBM). Owing to the use of DSBM in the novel scheme, the cost-effectiveness and the stability of the OPCR are essentially enhanced. The working principle and the theoretical analysis are demonstrated. Experiment is conducted to verify that the performance of the DSBM-based OPCR is comparable with that based on single sideband modulation. Large measurement range over 58 km with high spatial resolution of 10 cm is experimentally achieved.**

***Index Terms*— Fiber optics sensors, frequency modulation, optical time domain reflectometry.**

I. Introduction

OPTICAL time domain reflectometry (OTDR) [1], [2] and optical frequency domain reflectometry (OFDR) [3]–[5] have been widely studied. Though their performance is predecessor, limitations still exist. The spatial resolution of OTDR is directly related to the pulse width. Higher spatial resolution needs narrower pulse width, but a narrow pulse width decreases the power of detecting light and limits the dynamic range [6]. OFDR can alleviate the tradeoff via employing a continuous linear frequency modulated light as the source, which makes the spatial resolution determined by sweeping bandwidth. Its measurement range, however, is limited by the half of the laser source's coherent length [7]. Moreover, optical coherence domain reflectometry (OCDR) [8] and optical low coherence reflectometry (OLCR) [9] can also provide competitive spatial resolution but the measurement range is confined as well. To break the above limitations, a novel reflectometry technology based on a linear frequency modulation (LFM) pulse, called optical pulse compression reflectometry (OPCR) [10], [11], was proposed. The matching filter compresses the backscattered frequency-modulated pulse based on the pulse compression technology [12]. The spatial resolution is determined by the compressed pulse width since the backscatter is measured in time domain, which breaks the limitation between spatial resolution and dynamic range. Also, the pulse compression technology has higher resistance to the phase noise than OFDR [10], so OPCR can detect a fiber comparable to or even longer than the coherent length of light source. To date, OPCR can achieve 10 cm spatial resolution over 5.4 km measurement range using a laser source with a coherent length of 2 km and an LFM pulse with instantaneous sweeping bandwidth of 1 GHz [11].

From the viewpoint of implementation, the pulse in OTDR can be generated by the optical switch or modulation and the continuous frequency modulated light in OFDR can be realized by tunable light source [4], external phase [13] or amplitude [14] modulator. Besides, the advantage of single sideband modulation (SSBM) over double sideband modulation (DSBM) in OFDR was also verified [14] since DSBM enables the detected beat signal zero at some particular locations and restricts its feasibility. In early studies [10], [11], OPCR uses SSBM to generate frequency-modulated pulse. Since there are three bias voltages needed to be precisely adjusted in SSBM to suppress optical carrier and another sideband [14], [15], the system complexity and cost are high and the measurement performance is easily influenced by the bias voltage fluctuation.

In this letter, we report an OPCR based on DSBM so as to overcome the problems mentioned above. Obviously, the cost of DSBM is lower than SSBM. Moreover, there is only one bias voltage to be controlled in DSBM whereas three bias voltages are required to be precisely controlled. Compared with the previous scheme of OPCR based on SSBM [10], the DSBM-based OPCR system is more cost-effective, more stable, and less complicated. The working principle is demonstrated. The numerical simulation is given to prove the feasibility. And an experimental verification with 58-km measurement range and 10-cm spatial resolution is implemented.

II. Principle and Experimental Setup

The basic configuration of OPCR [10] requires a laser source to be split into two branches: one is modulated with an LFM pulse and the other serves as the local reference light. When a continuous light is launched into a DSBM or a Mach-Zehnder modulator (MZM), it is reasonable to assume

Manuscript received September 29, 2015; revised December 9, 2015; accepted December 30, 2015. Date of publication January 1, 2016; date of current version February 25, 2016. This work was supported in part by the National Natural Science Foundation of China under Grant 61535006 and Grant 61571292, in part by the Specialized Research Fund within the Doctoral Program through the Ministry of Education under Grant 20130073130005, in part by the State Key Laboratory Project of Shanghai Jiao Tong University under Grant 2014ZZ03016, and in part by Shanghai Key Laboratory of Specialty Fiber Optics and Optical Access Networks (Grant SKLSFO2015-04). *(Corresponding author: Weiwen Zou.)*

The authors are with the State Key Laboratory of Advanced Optical Communication Systems and Networks, Shanghai Jiao Tong University, Shanghai 200240, China, and also with the Shanghai Key Laboratory of Navigation and Location Services, Shanghai Jiao Tong University, Shanghai 200240, China (e-mail: ylei3stone@sjtu.edu.cn; wzou@sjtu.edu.cn; jpchen62@sjtu.edu.cn).

Color versions of one or more of the figures in this letter are available online at http://ieeexplore.ieee.org.

Digital Object Identifier 10.1109/LPT.2015.2514107

that only the first-order modulated sidebands are considerable. So the detecting modulated pulse E_p can be expressed by [14]

$$E_p(t) = \text{rect}\left(\frac{t}{T}\right)\left\{\begin{array}{l}\exp\left(j\omega_c t + j\omega_0 t + j\pi K t^2\right) \\ \quad + \exp\left(j\omega_c t - j\omega_0 t - j\pi K t^2\right)\end{array}\right\} \quad (1)$$

where $rect(\cdot)$ denotes the rectangular function, T is the pulse width, ω_c is the center angular frequency of optical carrier (laser), ω_0 is the start angular frequency of LFM, and K is the LFM slope.

The modulated pulse is launched into the fiber under test (FUT) and generates backscattered light. The backscatter is coherently detected with the local reference light. By use of a balanced photodetector (PD), namely the heterodyne detection [10], the electrical field of the backscatter is measured and later I/Q demodulated in digital domain. Later, the I/Q demodulated signal goes through a matching filter to recover the backscatter of Rayleigh scattering and/or end reflection in an FUT [10]. The recovered backscatter can be expressed by

$$y(t) = A(t) * \left\{rect\left(\frac{t}{2T}\right)\frac{T\sin\left[\pi K\left(T - |t|\right)(t)\right]}{\pi K T(t)}\right\} \quad (2)$$

where the symbol of "*" denotes the convolution operation and $A(t)$ corresponds to the backscatter of Rayleigh scattering occurring anywhere in the fiber, splicing loss at particular points, and end reflection due to Fresnel reflection. In the SSBM-based or DSBM-based OPCR system, $A(t)$ can be respectively expressed by

$$\begin{aligned} A_S(t) &= \Re \cdot r(t)\exp\left(-j\omega_c t\right) \\ A_D(t) &= \Re \cdot r(t)\cos\left(\omega_c t\right) \end{aligned} \quad (3)$$

where R corresponds to the total response of PD, the amplitude of modulated pulse and local reference light. $r(t)$ is the amplitude function determined by Rayleigh scattering and loss in the fiber. t denotes different time delays, corresponding to the position (z) along the FUT. Eq. (2) and Eq. (3) show that DSBM doesn't change the main lobe width of the compressed pulse, and the spatial resolution of OPCR is determined by the main lobe width [10]. So the spatial resolution of the DSBM-based OPCR can be expressed as follows [10]

$$\Delta z = \frac{c}{2nB} \quad (4)$$

where c is the light speed in vacuum, n is the refractive index of the FUT and B is the bandwidth of modulated pulse.

The difference between $A_S(t)$ and $A_D(t)$ is determined by the optical carrier (ω_c). In the SSBM-based OPCR, there is only one sideband. After coherent detection and I/Q demodulation, the phase change at different time delay remains an exponential form of $[exp(-j\omega_c t)]$. In the DSBM-based OPCR, two sidebands are coherently detected with the same reference signal. Two beat signals with opposite values of carrier's phase change are generated, leading to the cosine function in Eq. (3) and indicating that the amplitude of $A(t)$ oscillates at the carrier frequency ω_c with respect to the time delay t or the position z. In other words, there are some particular positions, where the amplitude of A_D is small or null. When there is a reflection at this null position, this event cannot be correctly observed although the total backscatter is an integration of the continuous Rayleigh backscattering and Fresnel reflections [see Eq. (1)]. Thus, it might be an error in the reflection measurement.

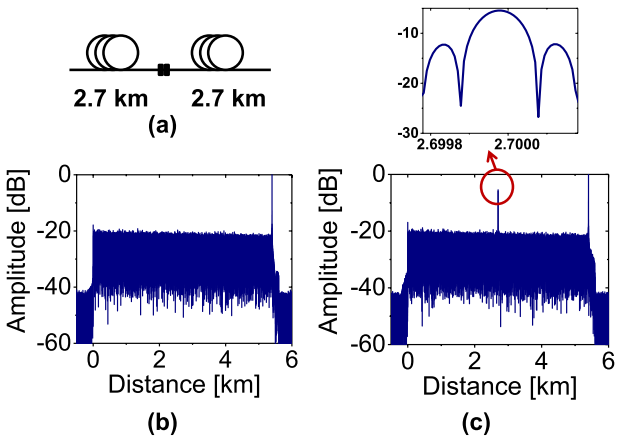

Fig. 1. Numerical simulation of DSBM based OPCR. (a) FUT structure. (b) Backscattering curve with the monochromatic laser source. (c) Backscattering curve considering the linewidth of laser source. The inset is the magnified peak at 2.7km.

However, the above theory only considers a monochromatic carrier. In fact, the laser source always has its linewidth and phase noise [7], [16], [17]. For more accurate analysis, the expression of optical carrier should include the phase jitter $\phi(t)$. The amplitude of backscatter $A'(t)$ in the DSBM-based OPCR is rewritten by

$$A'(t) = \Re \cdot r(t)\cos\left(\omega_c t + \varphi(t) - \varphi(t-\tau)\right) \quad (5)$$

In a continuous laser source, the phase noise $\phi(t)$ can be regarded as a random process and the values at different time are mutually independent. The phase difference $\Delta\phi = \phi(t) - \phi(t-\tau)$ can be treated as a random variable. According to Eq. (5), the carrier's frequency isn't a fixed value because of the phase noise and the position where the amplitude of A_D is null becomes uncertain. Consequently, the measurement error caused by position-dependent amplitude fluctuation is essentially reduced.

Figure 1 depicts the numerical simulation of the influence of phase noise on the reflection measurement. The laser's linewidth is assumed to be 100 kHz, the width of modulated pulse is 2 μs and the sweeping bandwidth is 1 GHz. The FUT is a ~2.7 km fiber spool connected with another ~2.7 km fiber spool [see Fig. 1(a)]. There are two reflection peaks caused by Fresnel reflection. As shown in Fig. 1(b), only one peak is detectable if the carrier frequency is monochromatic. This is because the time delay corresponding to the position of 2.7 km makes the phase close to $n\pi/2$ (n is an odd integer). According to Eq. (3), the reflection amplitude at 2.7 km is null. In contrast, if the linewidth of laser source is considered, the suppressed peak appears [see Fig. 1(c)], which indicates that the refection suppression is weakened.

The experimental setup of the DSBM-based OPCR is depicted in Fig. 2. A 1550 nm distributed feedback laser diode (NEL Ltd.) with ~100 kHz linewidth [10] and another laser (FM Photonics Ltd.) with ~3 kHz linewidth are used as the

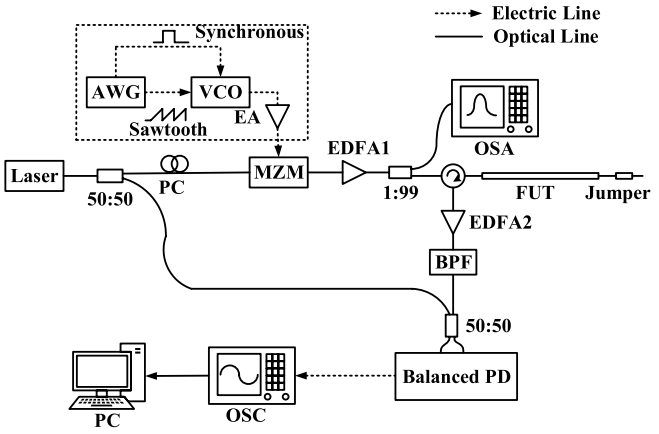

Fig. 2. Experimental setup of the DSBM-based OPCR. AWG: arbitrary waveform generator, VCO: voltage control oscillator, EA: electrical amplifier, PC: polarization controller, MZM: Mach-Zehnder modulator, EDFA: Erbium-doped fiber amplifier, OSA: optical spectrum analyzer, BPF: bandpass filter, OSC: oscilloscope.

optical source, respectively. A VCO (Mini-Circuits Ltd.) with 1-GHz sweeping range after an electrical amplifier (EA) is driven by a sawtooth wave to generate LFM microwave pulse. It modulates a MZM (EOSPACE Ltd.) so as to generate DSBM with optical carrier suppression. The polarization state and bias voltage of MZM are properly adjusted and its output is monitored by an optical spectrum analyzer (OSA, Yokogawa Ltd.). An erbium-doped fiber amplifier (EDFA) lays behind MZM to compensate its loss.

The backscatter is coherently detected with the local reference light and then converted into the electrical signal by a balanced PD (Discovery DSC720) with 16-GHz bandwidth. The digitalization is employed by an oscilloscope (Tektronix DSA 70804), the I/Q demodulation and matching filter are digitally fulfilled by a computer. When the FUT becomes longer, the backscatter contains less reflection of the LFM pulse due to fiber loss. In order to overcome this problem, another EDFA and an optical bandpass filter (BPF) are laid before the PD so as to increase the effective signal power. In order to verify the spatial resolution, a 15 cm jumper is always connected at the end of the FUT with different length. The connection is not strictly tight so that both ends of the jumper generate Fresnel reflection, creating two reflection peaks with an interval of 15 cm.

III. Results and Discussion

The measured backscatter of ~10 km FUT with 100-kHz-linewidth laser diode is depicted in Fig. 3(a). The overall curve demonstrates that the DSBM-based OPCR can successfully detect the reflections at the far end of 10 km. Since the sweep range is 1 GHz, the nominal spatial resolution is 10 cm according to Eq. (4) and $n = 1.448$ in single mode fiber. At the near end of FUT, a reflection peak is depicted in Fig. 3(b). The full width at half magnitude (FWHM) of the main lobe is 10 cm, which agrees with the nominal value. As illustrated in Fig. 3(c), there are two well-interrogated peaks with 15-cm interval, corresponding to the far end of the FUT or the jumper. It further verifies the 10-cm spatial resolution of the DSBM-based OPCR.

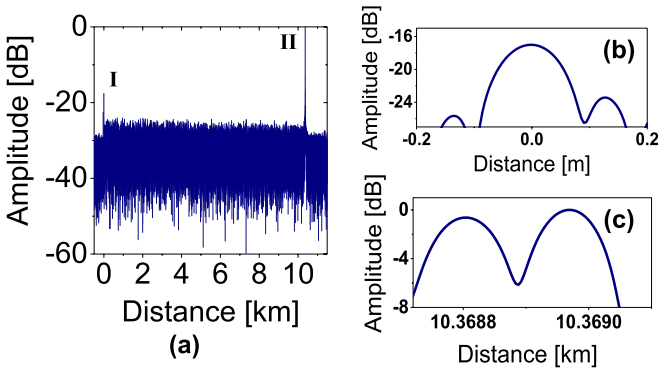

Fig. 3. Experimental result of 10 km testing fiber. (a) Overall backscattering curve. (b) Magnified curve of reflection peak at near end of 10 km FUT. (c) Magnified curve at the far end of FUT.

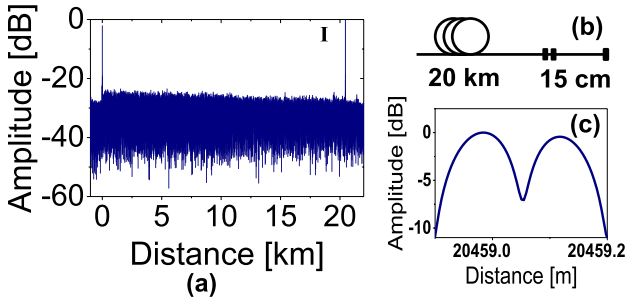

Fig. 4. (a) Overall backscattering curve of 20 km FUT. (b) The structure of FUT. (c) Magnified curve at far end of FUT.

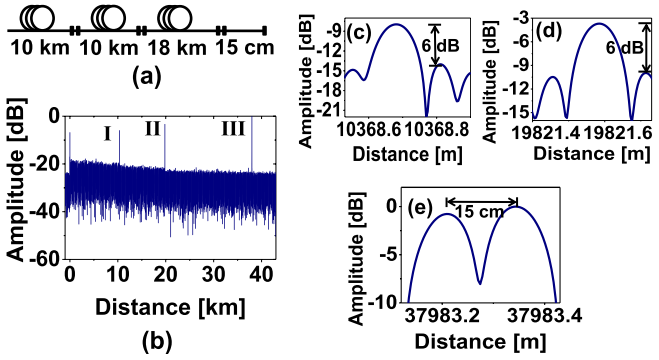

Fig. 5. (a) Configuration of 38 km FUT. (b) Overall backscattering curve. (c) Magnified curve at "I" position of (b). (d) Magnified curve at "II" position of (b). (e) Magnified curve at "III" position of (b).

The 3-kHz-linewidth laser source is substituted to test three other FUTs with longer fiber lengths of 20 km, 38 km, and 58 km, respectively.

As depicted in Fig. 4(a) the reflection peaks in the 20-km FUT [see Fig. 4(b)] are interrogated and the fiber loss is recognized. At the far end of FUT, two reflection peaks of the jumper magnified in Fig.4 (c) are well identified with 15-cm interval. For the 38-km FUT [see Fig. 5(a)], the connections of three fiber spools are detected [see Fig. 5(b)]. As zoomed-in in Fig. 5(c) and 5(d), the main peaks in the middle of the FUT are 6 dB higher than the side lobes. Besides, two peaks separated by 15 cm [see Fig. 5(e)] indicate that the 10-cm spatial

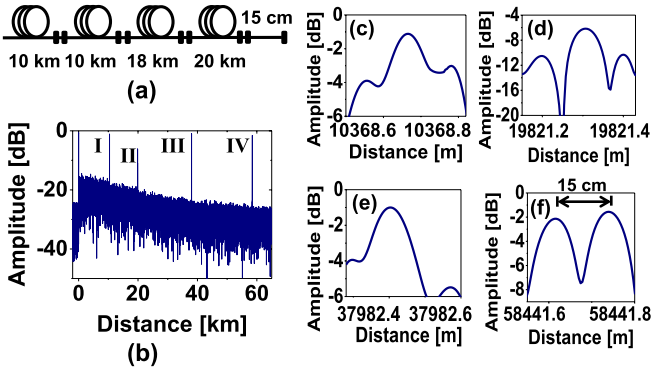

Fig. 6. (a) Configuration of 58 km FUT. (b) Overall backscattering curve. (c) Magnified curve at "I" position of (b). (d) Magnified curve at "II" position of (b). (e) Magnified curve at "III" position of (b). (f) Magnified curve at "IV" position of (b).

resolution is guaranteed. Furthermore, the measurement results in the 58-km FUT comprising four fiber spools and the 15-cm jumper are summarized in Fig. 6. It verifies the measurement ability of 58-km measurement range [see Fig. 6(b)] and 10-cm spatial resolution since the fiber connectors [see Fig. 6(c)-(e)] and fiber jumper [see Fig. 6(f)] can be well interrogated. Figure 6(b) shows that the rear part of backscatter has very gentle slope, this is because the longer the fiber increases, the lower ratio of Rayleigh scattering in total backscatter signal, which makes the Rayleigh scattering buried in noise. To overcome this, more times averaging can be used as in [10].

IV. Conclusion

In the present work we have presented that the DSBM is a new cost-effective solution for OPCR, which was impossible in OFDR [14]. The theoretical and experimental analysis indicates that the DSBM-based OPCR enables reflection interrogation at null positions due to the intrinsic linewidth of laser source. In the experiment, 58 km measurement range with 10 cm spatial resolution is successfully demonstrated.

Acknowledgment

We thank the FM Photonics Company for lending us the narrow linewidth laser.

References

[1] X. Bao and L. Chen, "Recent progress in distributed fiber optic sensors," *Sensors*, vol. 12, no. 7, pp. 8601–8639, Jun. 2012.
[2] M. K. Barnoski, M. D. Rourke, S. M. Jensen, and R. T. Melville, "Optical time domain reflectometer," *Appl. Opt.*, vol. 16, no. 9, pp. 2375–2379, Mar. 1977.
[3] W. Eickhoff and R. Ulrich, "Optical frequency domain reflectometry in single-mode fiber," *Appl. Phys. Lett.*, vol. 39, no. 9, pp. 693–695, Aug. 1981.
[4] D. Uttam and B. Culshaw, "Precision time domain reflectometry in optical fiber systems using a frequency modulated continuous wave ranging technique," *J. Lightw. Technol.*, vol. 3, no. 5, pp. 971–977, Oct. 1985.
[5] B. J. Soller, D. K. Gifford, M. S. Wolfe, and M. E. Froggatt, "High resolution optical frequency domain reflectometry for characterization of components and assemblies," *Opt. Exp.*, vol. 13, no. 2, pp. 666–674, Jan. 2005.
[6] M. Nazarathy *et al.*, "Real-time long range complementary correlation optical time domain reflectometer," *J. Lightw. Technol.*, vol. 7, no. 1, pp. 24–38, Jan. 1989.
[7] S. Venkatesh and W. V. Sorin, "Phase noise considerations in coherent optical FMCW reflectometry," *J. Lightw. Technol.*, vol. 11, no. 10, pp. 1694–1700, Oct. 1993.
[8] M. Kashiwagi and K. Hotate, "Long range and high resolution reflectometry by synthesis of optical coherence function at region beyond the coherence length," *IEICE Electron. Exp.*, vol. 6, no. 8, pp. 497–503, Aug. 2009.
[9] S. Li, X. Li, W. Zou, and J. Chen, "Rangeability extension of fiber-optic low-coherence measurement based on cascaded multistage fiber delay line," *Appl. Opt.*, vol. 51, no. 6, pp. 771–775, Feb. 2012.
[10] W. Zou, S. Yang, X. Long, and J. Chen, "Optical pulse compression reflectometry: Proposal and proof-of-concept experiment," *Opt. Exp.*, vol. 23, no. 1, pp. 512–522, Jan. 2015.
[11] W. Zou, S. Yang, X. Long, and J. Chen, "Optical pulse compression reflectometry with 10 cm spatial resolution based on pulsed linear frequency modulation," in *Proc. Opt. Fiber Commun. Conf.*, 2015, p. W3I.5.
[12] M. A. Richards, *Fundamentals of Radar Signal Processing*. New York, NY, USA: McGraw-Hill, 2005.
[13] K. Tsuji, K. Shimizu, T. Horiguchi, and Y. Koyamada, "SPATIAL-resolution improvement in long-range coherent optical frequency-domain reflectometry by frequency-sweep linearization," *Electron. Lett.*, vol. 33, no. 5, pp. 408–410, Feb. 1997.
[14] Y. Koshikiya, X. Fan, and F. Ito, "Long range and cm-level spatial resolution measurement using coherent optical frequency domain reflectometry with SSB-SC modulator and narrow linewidth fiber laser," *J. Lightw. Technol.*, vol. 26, no. 18, pp. 3287–3294, Sep. 15, 2008.
[15] M. Izutsu, S. Shikama, and T. Sueta, "Integrated optical SSB modulator/frequency shifter," *IEEE J. Quantum Electron.*, vol. 17, no. 11, pp. 2225–2227, Nov. 1981.
[16] J. A. Armstrong, "Theory of interferometric analysis of laser phase noise," *J. Opt. Soc. Amer.*, vol. 56, no. 8, pp. 1024–1028, Feb. 1966.
[17] R. W. Tkach and A. R. Chraplyvy, "Phase noise and linewidth in an InGaAsP DFB laser," *J. Lightw. Technol.*, vol. 4, no. 11, pp. 1711–1716, Nov. 1986.